# Performance Evaluation of a MEMS Compact Electrostatic Microgripper Equipped with Rotary Comb Drives and Curved Flexure Hinges

Lorenzo Giannini*, Alessio Buzzin*, Gabriele Bocchetta**, Rita Asquini*, Andrea Scorza**, Giampiero de Cesare*, and Nicola Pio Belfiore**
* Department of Information Engineering, Electronics and Telecommunications, Sapienza University of Rome, Rome, Italy
** Department of Industrial, Electronic and Mechanical Engineering, Roma Tre University
lorenzo.giannini@uniroma1.it

***Abstract*—Microgrippers can be conveniently designed and built as MEMS-Technology based devices for handling and manipulating objects at a microscopic scale. In this work is presented a microgripper equipped with curved flexure hinges. The design is specifically studied to improve its grasping capabilities with respect to those found in literature, while maintaining a small overall footprint of 20 mm$^2$, and a well established fabrication procedure (Silicon-On-Insulator technology). The microgripper is electrostatically actuated through five rotary comb-drives made of interdigitated fingers. Finite Element Analysis has been adopted to analyze the system performance when voltage is applied.**
**As main figures of merit, the tip displacement and rotation, the maximum stress sustained by the flexure hinges and the maximum operating voltage (MOV) are investigated. A tip displacement up to 39 μm and a tip rotation of about 1° were achieved at 15 V of MOV, better than other electrostatically driven microgrippers presented in literature. Such microgripper enables the manipulation of objects with size ranging from a few microns to tens of microns requiring relatively low voltage, thus suggesting its use in the field of integrated micromanipulation and micro-surgery.**

***Keywords—Microgrippers, MEMS, electrostatic actuators, Silicon-On-Insulator, finite element analysis, compliant mechanisms.***

## I. Introduction

Over the last years, there has been an increase in demand for devices having as main features high accuracy and precise motion control with the aim of manipulating objects of micrometric size [1], [2]. Design, fabrication, and control of microsystems for micromanipulation encountered several challenges since, at the micro or nano scale levels, many paradigms fundamental to macro-scale engineering are no longer applicable [3]. Thanks to the development of microelectromechanical systems (MEMS) and the implementation of technologies derived from microelectronics many of these issues are nowdays overcome [4]–[7]. Among all the solutions available for micromechanisms, research has focused on the development of microgrippers capable of manipulating and grasping microscopic objects (1-100μm) [8]. These devices are widely investigated as potential tools for various applications, such as minimally invasive surgery [9], [10], drug delivery [11], [12] and tissue engineering [13]. In recent years, MEMS microgrippers with diverse shapes, actuation mechanisms, and sensing principles have been developed [14], [15]. Actuation plays a crucial role as it must provide the required force/torque to complete the desired task. The literature features microgrippers making use of several kinds of actuation, such as electro-thermal [16], piezoelectric [17], shape memory [18], etc. This paper focuses on electrostatic actuation because of its rapid time response, straightforward design, extensive versatility, and low power consumption [19], [20]. In this work, a novel and compact electrostatic microgripper is presented, designed to offer accurate and wide gripping capabilities. The device relies on electrostatic forces for actuation, using rotary comb-drives to generate the required motion and is equipped with curved flexure hinges which increase the range of motion, widening the microgripper's adaptability to various shapes and sizes of target objects. Furthermore, implementing flexible beams as hinges [21], [22], monolithic devices can be achieved through a single lithographic step for the geometry definition [23]. The paper is arranged as follows. Section 2 outlines the microgripper under investigation, including its main features, operating principle, and manufacturing process. Section 3 describes the finite element analysis approach for estimating device's performances as a function of supply voltage. Finally, Section 4 reports and discusses the outcomes of numerical simulations on microactuator displacement and related gripper tip displacement, as well as stress analysis caused by bending hinge deformation.

## II. Design and Working Principle

The purpose of this work is to develop a voltage-driven microgripper able of achieve high actuation efficiency (i.e. large tip displacement with respect to the actuation voltage). Fig. 1a shows the schematic top view of the designed microgripper. From a kinematic standpoint, two movable links ("MOBILE", blue in figure) are connected to a fixed frame ("ANCHORED", gray in figure). The tips' total operating window is 120 × 150 μm$^2$. The movement takes place around two flexible curved beams

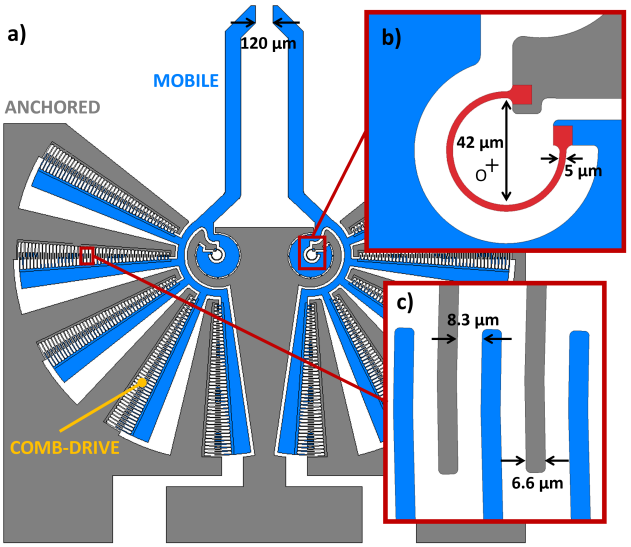


Fig. 1. Device's design. a) Schematic top view of the designed microgripper; (b) Enlargement on the curved flexure hinge design (red in figure); (c) Enlargement on the comb-drive fingers.

acting as rotary hinges (red in Fig. 1b) [24], [25]. These curved beams are shaped as circumferential arcs with a diameter of 42 µm and a width of 5 µm [26]. Using such hinges, it is possible to perform a rotational motion around the center of the beam's elastic weight ("O" in figure), when the device is actuated. The presented microgripper is operated by comb-drives, which are very common electrostatic actuators [27], combining design simplicity, precision, and rapid response time [28]. More specifically, the presented structure uses ten pairs of rotary comb-drives (five on each side), each made of 43 interdigitated fingers. This specific design is the result of extensive studies focused on the functional characterization of previous microgripper geometries, which confirmed that displacement is directly proportional to the number of active comb-drives [29]. Anchored fingers (gray in Fig. 1c) are fixed to the frame while suspended fingers (blue in Fig. 1c) can move in the direction of the fixed ones when a voltage is applied, due to electrostatic force. Every comb has 6.6µm-wide fingers and the gap between movable and fixed fingers is 8.3 µm (Fig. 1c). The comb-drive finger arrays have an initial overlap of 2° in rest position (i.e., 0 V applied). The device is designed to be fabricated using microelectronics fabrication techniques, on a Silicon-On-Insulator (SOI) substrate with a 40µm-thick device layer [30]. The design requirements suggested the use of monocrystalline silicon (Si) as a structural material, enabling a fabrication procedure based on a single photolithographic step for the geometry definition, and on Deep Reactive Ion Etching (DRIE) [31] for the patterning, as vertical sidewalls are necessary for hinge bending. The geometrical features of the device are summarized in Tab I.

## III. Numerical Analysis

The proposed study is based on simulations performed with the commercial software COMSOL Multiphysics®, incorporating Finite Element Analysis (FEA) to predict the system's electromechanical performance. This means to combine the "Solid Mechanics" physics module with the "Electrostatic" physics module to investigate the device's behavior when a voltage is applied. The FEA simulations were executed using a 2D model of the microgripper (considering 40 µm out-of-plane thickness) in order to reduce the computational efforts, and modelling the air surrounding the device as a free deforming domain to simulate the electrostatic actuation physics. To improve precision, a triangular mesh was refined in corresponding of the thinnest elements, resulting in approximately three million sub-domains. The simulations were carried out using a parametric sweep of the applied voltage from 0 V to 15 V with 1 V steps. The key factors is simulating the electrostatic actuation include the relative permittivity of the solid and dielectric medium, as well as the elastic modulus of the moving component. The presented simulation model has been recursively perfected in order to match with the outcomes of the experimental tests on similar structures previously studied [32], [33]. as a result, key attributes (such as the Young's modulus of Si [34]) were refined, allowing the implementation of a microgripper phy-digital twin, useful for the development and optimization of new designs.

## IV. Results

This section describes the outcomes from numerical analyses used to evaluate the performance of the novel electrostatic microgripper concept proposed in the present study. The section is separated into two subsections that address the displacement results as a function of supply voltage and actuation force, as well as the stress results. Table II highlights the key findings. It is worth noting that these simulations assessed the actuation force, considered as the force exerted by the comb-drives on the gripper structure for its motion, and it depends on the number and on the geometry of the comb fingers, and on the actuation voltage (i.e. the voltage applied to the anchored contact pads). It is important to distinguish the actuation force from

TABLE I
Geometrical features of the proposed microgripper.

| Component | Label | Value |
|---|---|---|
| Finger | Thickness | 40 µm |
| | Width | 6.6 µm |
| | Gap | 8.3 µm |
| | Initial overlapping angle | 2° |
| | Number per comb-drive | 43 |
| Hinge | Diameter | 42 µm |
| | Width | 5 µm |
| | Thickness | 40 µm |

the gripping force, which is the force exerted on an object being grasped by the gripper tips.

### A. Displacement Analysis

Fig. 2 shows results of the simulations carried out to study the motion of the presented device. Firstly, the displacement of the left tip is considered when a voltage is applied. A quadratic trend of the displacement can be identified when it is compared with the applied voltage (Fig. 2a). The inset of Fig. 2a shows the movement of the tip from his rest position (framed with no color filling) to the maximum displacement state (colored). Fig. 2b plots the linear relationship between tip displacement and force generated by the comb-drive actuation. A maximum displacement of 39 µm is achieved at 15 V applied voltage (corresponding to 2 µN of actuation force). When more than 15 V are applied, the comb-drive undergoes the pull-in phenomenon. The comb-drive rotation was also investigated. Fig. 3 shows the plots of the comb-drive rotation with respect to the applied voltage (Fig. 3a) and to the actuation force (Fig. 3b). As in the case of the tip displacement, the pattern is quadratic when considered as a function of voltage and linear when considered as a function of actuation force. The inset in Fig. 3a shows the rotation of one of the comb-drives, and it is worth noting that the same behavior belongs to each of the combs.

### B. Stress Analysis

The deformation due to the electrostatic actuation causes mechanical stresses and strains which must be carefully addressed with an additional study. Hereinafter is presented an analysis of the mechanical stress induced on the flexure hinges when applying a voltage. Fig. 4 shows the Maximum Tresca stress distribution located in the flexure hinge. When 15 V are applied, the Maximum Principal Stress (MPS) is equal to 4.83 MPa, which is three orders of magnitude smaller than the Si yield strength (6.9 GPa). This demonstrates how such structure is capable of withstanding the mechanical stresses induced by the applied voltage in the whole actuation range without exceeding its structural limits, avoiding damages and ruptures. Tab. III shows a comparison between the performances of the presented device with respect to those of other solutions found in literature. The main performances analyzed are the achievable total tip displacement ($\delta$) of the device, evaluated as a function of the total footprint of the device (that refers to the physical space or area that the microgripper occupies on a surface), the Maximum Operating Voltage (MOV), that is the maximum value of actuation voltage applicable before reaching the pull-in state [35], and the actuation force ($F_{act}$). Tab. III highlights how the presented device displays a $\delta$ comparable with the others, with lower MOV and $F_{act}$. The actuation efficiency ($\eta$) is calculated as the ratio between $\delta$ and MOV, and refers to the device's ability to convert the applied electrical energy, in the form of voltage, into a desired mechanical motion, as measured by the displacement of the microgripper tip. Here, the achievement of a significantly larger $\eta$ with respect to other designs is clearly notable.

TABLE II
SUMMARY OF THE MAXIMUM VALUES OBTAINED FROM NUMERICAL SIMULATION.

| Parameter | Value |
|---|---|
| Actuation Force (µN) | 2 |
| Comb-drive rotation (°) | 1 |
| Tip displacement (µm) | 39 |
| Hinge stress (MPa) | 4.83 |

## V. CONCLUSIONS

This paper presents a microgripper designed to achieve large tip displacements when subjected to a an applied

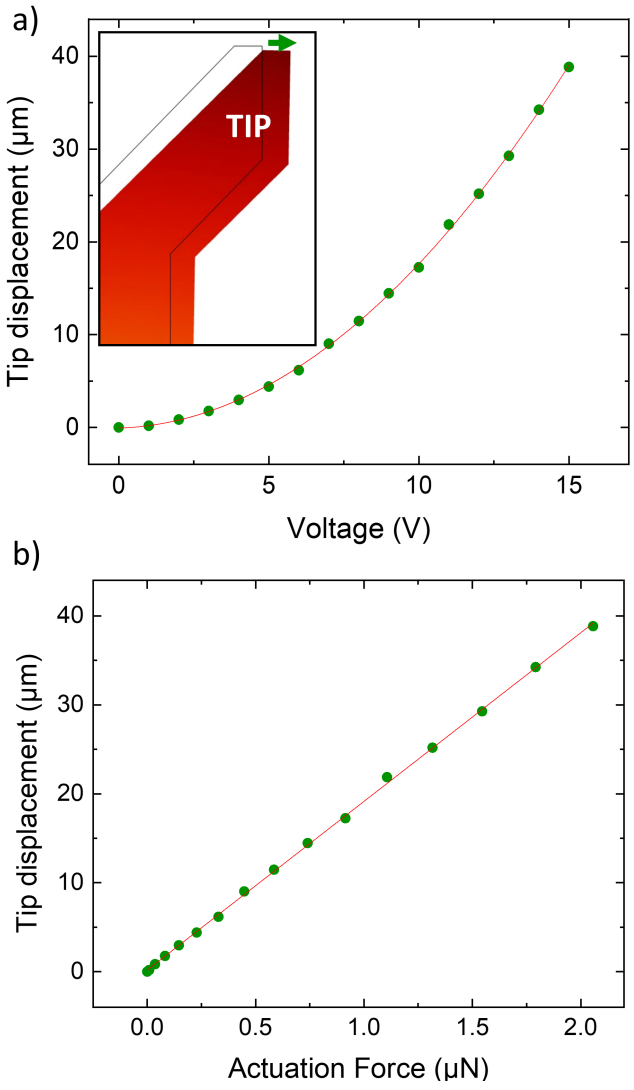


Fig. 2. a) Plot of the tip displacement with respect to the applied voltage. The inset shows the movement (green arrow) of the TIP from his rest position (transparent) to the position reached at 15 V (colored). b) Plot of the tip displacement with respect to the actuation force.

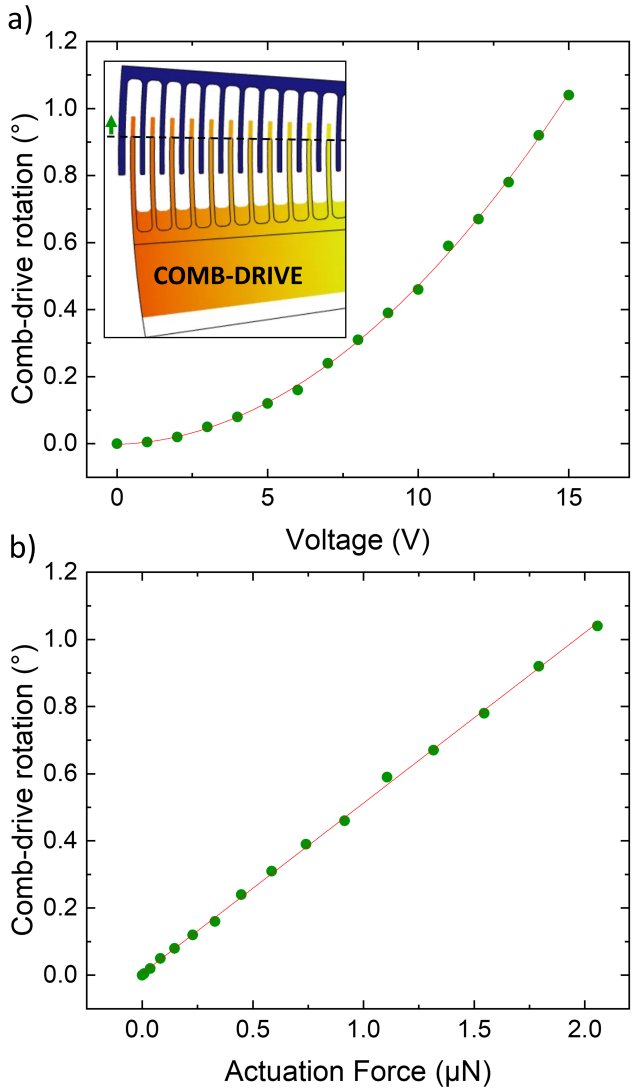


Fig. 3. a) Plot of the comb-drive rotation with respect to the applied voltage. The inset shows the rotation (green arrow) of the comb-drive from his rest position (transparent) to the position reached at 15 V (colored). b) Plot of the comb-drive rotation with respect to the actuation force.

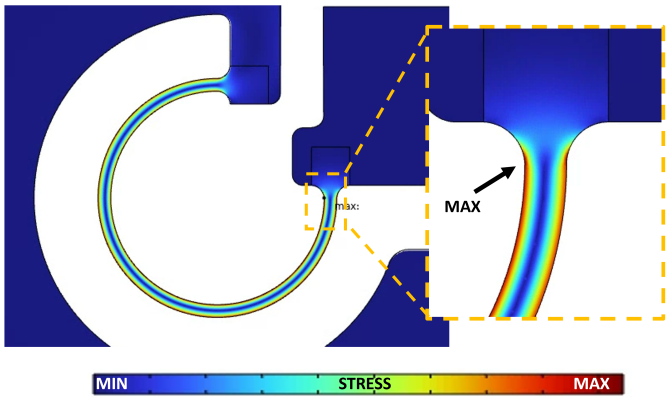


Fig. 4. Maximum Principal Stress (MPS) located in the flexure hinge

TABLE III
COMPARISON OF DIFFERENT ELECTROSTATIC MICROGRIPPER OPERATING DISPLACEMENT

| Design | Footprint ($\mu m^2$) | MOV (V) | $F_{act}$ (μN) | $\delta$ (μm) | $\eta$ (μm/V) |
|---|---|---|---|---|---|
| Beyeler et al. [36] | 7700x5600 | 150 | 493 | 50 | 0.33 |
| Volland et al. [37] | 1250x3300 | 80 | 115.5 | 20 | 0.25 |
| Wang et al. [38] | 3700x3700 | 40 | 25.5 | 36.45 | 0.91 |
| Vurchio et al. [39] | 2710x4417 | 24 | 6.8 | 31 | 1.29 |
| Proposed device* | 4540x4416 | 15 | 2 | 39 | 2.60 |

*From COMSOL simulations

voltage. Simulation results show that the microgripper is able to reach tip displacements of 39 μm when a voltage of 15 V is applied. This result is noteworthy, as the microgripper demonstrates high actuation efficiency with respect to other devices found in literature with similar footprint (see Tab. III). With regard to the mechanical stress analysis, the device maintains its mechanical integrity, as the MPS at the MOV is always kept orders of magnitude below Si yield strength, thus being able to handle the stresses induced by electrostatic actuation. The proposed microgripper design shows promising performance in achieving relatively larger tip displacements with relatively lower applied voltage in comparison with the grippers presented in literature, demonstrating also structural reliability. The results encourage further developments and future implementation in applications when relatively low voltage is preferred for actuation, such as in the fields of biological manipulation.

## REFERENCES

[1] N. P. Belfiore, "Micromanipulation: A challenge for actuation," 2018.
[2] M. A. Rahman and A. T. Ohta, "Micromanipulation with microrobots," 2021.
[3] B. Bhushan, "Springer Handbook of Nanotechnology," *Sensor Review*, vol. 24, no. 3, 2004.
[4] M. Gad-el Hak, *The MEMS Handbook: Applications*, 2006, vol. 23.
[5] M. Gadola, F. Maspero, G. Langfelder, M. Sansa, T. Verdot, A. Berthelot, and P. Robert, "50-kHz MEMS gyroscopes based on NEMS sensing with 1.3 mdps/Hz ARW and 0.5°/h stability," in *Proceedings of IEEE Sensors*, vol. 2020-October, 2020.
[6] R. Della Sala, F. Centurelli, G. Scotti, and G. Palumbo, "Rail to rail icmr and high performance ulv standard-cell-based comparator for biomedical and iot applications," *IEEE Access*, 2024.
[7] M. Barbirotta, A. Cheikh, A. Mastrandrea, F. Menichelli, M. Angioli, S. Jamili, and M. Olivieri, "Fault-Tolerant Hardware Acceleration for High-Performance Edge-Computing Nodes," *Electronics (Switzerland)*, vol. 12, no. 17, 2023.
[8] F. Vurchio, P. Ursi, A. Buzzin, A. Veroli, A. Scorza, M. Verotti, S. A. Sciuto, and N. P. Belfiore, "Grasping and releasing agarose micro beads in water drops," *Micromachines*, vol. 10, no. 7, 2019.
[9] H. Ceylan, J. Giltinan, K. Kozielski, and M. Sitti, "Mobile microrobots for bioengineering applications," 2017.
[10] G. Bao and S. Suresh, "Cell and molecular mechanics of biological materials," 2003.
[11] M. Power, A. J. Thompson, S. Anastasova, and G. Z. Yang, "A Monolithic Force-Sensitive 3D Microgripper Fabricated on the Tip of an Optical Fiber Using 2-Photon Polymerization," *Small*, vol. 14, no. 16, 2018.

[12] M. Elango and A. Annamalai, "Design and Analysis of Microgripper Using COMSOL for Drug Delivery Applications," in *Springer Proceedings in Materials*, 2021, vol. 9.
[13] K. Inoue, T. Arai, T. Tanikawa, and K. Ohba, "Dexterous micromanipulation supporting cell and tissue engineering," in *Proceedings of the 2005 International Symposium on Micro-NanoMechatronics and Human Science, Eighth Symposium on Micro- and Nano-Mechatronics for Information-Based Society - The 21st Century COE Progr*, vol. 2005, 2005.
[14] Z. Lyu and Q. Xu, "Recent design and development of piezoelectric-actuated compliant microgrippers: A review," 2021.
[15] S. Yang and Q. Xu, "A review on actuation and sensing techniques for MEMS-based microgrippers," 2017.
[16] A. Somà, S. Iamoni, R. Voicu, R. Müller, M. H. Al-Zandi, and C. Wang, "Design and experimental testing of an electro-thermal microgripper for cell manipulation," *Microsystem Technologies*, vol. 24, no. 2, 2018.
[17] Y. L. Yang, Y. D. Wei, J. Q. Lou, G. Tian, X. W. Zhao, and L. Fu, "A new piezo-driven microgripper based on the double-rocker mechanism," *Smart Materials and Structures*, vol. 24, no. 7, 2015.
[18] A. Abuzaiter, M. Nafea, and M. S. Mohamed Ali, "Development of a shape-memory-alloy micromanipulator based on integrated bimorph microactuators," *Mechatronics*, vol. 38, 2016.
[19] A. Buzzin, A. Rossi, E. Giovine, G. de Cesare, and N. P. Belfiore, "Downsizing Effects on Micro and Nano Comb Drives," *Actuators*, vol. 11, no. 3, pp. 1–13, 2022.
[20] I. Morkvenaite-Vilkonciene, V. Bucinskas, J. Subaciute-Zemaitiene, E. Sutinys, D. Virzonis, and A. Dzedzickis, "Development of Electrostatic Microactuators: 5-Year Progress in Modeling, Design, and Applications," 2022.
[21] A. Cammarata, P. D. Maddio, R. Sinatra, and N. P. Belfiore, "Direct Kinetostatic Analysis of a Gripper with Curved Flexures," *Micromachines*, vol. 13, no. 12, 2022.
[22] N. Lobontiu, J. Hunter, J. Keefe, and J. Westenskow, "Tripod mechanisms with novel spatial Cartesian flexible hinges," *Mechanism and Machine Theory*, vol. 167, 2022.
[23] M. Verotti, R. Crescenzi, M. Balucani, and N. P. Belfiore, "MEMS-based conjugate surfaces flexure hinge," *Journal of Mechanical Design*, vol. 137, no. 1, pp. 1–10, 2015.
[24] N. Lobontiu, *Compliant mechanisms: Design of flexure hinges*, 2002.
[25] A. Cammarata, P. D. Maddìo, R. Sinatra, A. Rossi, and N. P. Belfiore, "Dynamic model of a conjugate-surface flexure hinge considering impacts between cylinders," *Micromachines*, vol. 13, no. 6, 2022. [Online]. Available: https://www.mdpi.com/2072-666X/13/6/957
[26] A. Buzzin, L. Giannini, G. Bocchetta, A. Notargiacomo, E. Giovine, A. Scorza, R. Asquini, G. D. Cesare, and N. P. Belfiore, "On the Dependency of the Electromechanical Response of Rotary MEMS / NEMS on Their Embedded Flexure Hinges ' Geometry," *Micromachines*, vol. 14, no. 12, 2023.
[27] A. S. Algamili, M. H. M. Khir, J. O. Dennis, A. Y. Ahmed, S. S. Alabsi, S. S. Ba Hashwan, and M. M. Junaid, "A Review of Actuation and Sensing Mechanisms in MEMS-Based Sensor Devices," *Nanoscale Research Letters*, vol. 16, no. 1, 2021. [Online]. Available: https://doi.org/10.1186/s11671-021-03481-7
[28] A. Veroli, A. Buzzin, F. Frezza, G. de Cesare, M. Hamidullah, E. Giovine, M. Verotti, and N. P. Belfiore, "An approach to the extreme miniaturization of rotary comb drives," *Actuators*, vol. 7, no. 4, pp. 1–11, 2018.
[29] G. Bocchetta, G. Fiori, A. Scorza, N. P. Belfiore, and S. A. Sciuto, "First results on the functional characterization of two rotary comb-drive actuated MEMS microgripper with different geometry," in *25th IMEKO TC-4 International Symposium on Measurement of Electrical Quantities, IMEKO TC-4 2022 and 23rd International Workshop on ADC and DAC Modelling and Testing, IWADC 2022*, 2022.
[30] A. Bagolini, S. Ronchin, P. Bellutti, M. Chistè, M. Verotti, and N. P. Belfiore, "Fabrication of Novel MEMS Microgrippers by Deep Reactive Ion Etching With Metal Hard Mask," *Journal of Microelectromechanical Systems*, vol. 26, no. 4, pp. 926–934, 2017.
[31] A. Bagolini, P. Scauso, S. Sanguinetti, and P. Bellutti, "Silicon Deep Reactive Ion Etching with aluminum hard mask," *Materials Research Express*, vol. 6, no. 8, 2019.
[32] G. Bocchetta, G. Fiori, F. Filippi, P. Ursi, S. A. Sciuto, and A. Scorza, "First results on torque estimation by FEA and experimental analysis in a novel CSFH-based microgripper," *26th IMEKO TC4 International Symposium and 24th International Workshop on ADC/DAC Modelling and Testing*, no. 2, pp. 182–185, 2023.
[33] N. P. Belfiore, A. Bagolini, A. Rossi, G. Bocchetta, F. Vurchio, R. Crescenzi, A. Scorza, P. Bellutti, and S. A. Sciuto, "Design, fabrication, testing and simulation of a rotary double comb drives actuated microgripper," *Micromachines*, vol. 12, no. 10, pp. 1–21, 2021.
[34] M. A. Hopcroft, W. D. Nix, and T. W. Kenny, "What is the Young's modulus of silicon?" *Journal of Microelectromechanical Systems*, vol. 19, no. 2, 2010.
[35] W. M. Zhang, H. Yan, Z. K. Peng, and G. Meng, "Electrostatic pull-in instability in MEMS/NEMS: A review," 2014.
[36] F. Beyeler, A. Neild, S. Oberti, D. J. Bell, Y. Sun, J. Dual, and B. J. Nelson, "Monolithically fabricated microgripper with integrated force sensor for manipulating microobjects and biological cells aligned in an ultrasonic field," *Journal of Microelectromechanical Systems*, vol. 16, no. 1, 2007.
[37] B. E. Volland, H. Heerlein, and I. W. Rangelow, "Electrostatically driven microgripper," in *Microelectronic Engineering*, vol. 61-62, 2002, pp. 1015–1023.
[38] C. Wang, Y. Wang, W. Fang, X. Song, A. Quan, M. Gidts, H. Zhang, H. Liu, J. Bai, S. Sadeghpour, and M. Kraft, "Design of a large-range rotary microgripper with freeform geometries using a genetic algorithm," *Microsystems and Nanoengineering*, vol. 8, no. 1, 2022.
[39] F. Vurchio, F. Orsini, A. Scorza, and S. A. Sciuto, "Functional characterization of MEMS Microgripper prototype for biomedical application: Preliminary results," *Medical Measurements and Applications, MeMeA 2019 - Symposium Proceedings*, pp. 1–6, 2019.